Parasitology Research (2022) 121:3403–3415
https://doi.org/10.1007/s00436-022-07699-x

IMMUNOLOGY AND HOST-PARASITE INTERACTIONS - ORIGINAL PAPER

Clonorchis sinensis infection contributes to hepatocellular carcinoma progression in rat

Yapeng Qi[1] · Junwen Hu[1] · Jiahao Liang[1] · Xiaoyin Hu[1] · Ning Ma[2] · Bangde Xiang[1,3]

Received: 2 March 2022 / Accepted: 14 October 2022 / Published online: 21 October 2022

Abstract

Clonorchis sinensis (*C. sinensis*) infection is a risk factor for cholangiocarcinoma. Whether it also contributes to the development of hepatocellular carcinoma (HCC) is still unclear. This study explored the potential relationship between *C. sinensis* infection and HCC. A total of 110 Sprague–Dawley rats were divided into four treatment groups, the negative control group (NC) received intragastric (i.g.) administration of saline, while the clonorchiasis group (CS) received i.g. administration of 150 *C. sinensis* metacercariae. The diethylnitrosamine-induced group (DEN) received intraperitoneal (i.p.) administration of DEN. The clonorchiasis DEN-induced group (CSDEN) received i.g. administration of 150 *C. sinensis* metacercariae followed by i.p. administration of DEN. Hematoxylin and eosin staining, immunohistochemistry, and Masson's trichrome staining were performed for histopathological analysis of the isolated tissues. RNA-seq technology and RT-PCR were employed for gene expression. In the DEN group, 15 rats survived, of which 9 developed liver cirrhosis and 7 developed HCC. In the CSDEN group, all of the 17 surviving rats developed cirrhosis, and 15 showed development of HCC. The incidence of liver cirrhosis and HCC was significantly higher in the CSDEN group than in the DEN group. KEGG pathway analysis of the differentially expressed genes suggested significant upregulation in inflammation-associated pathways. Immunohistochemistry and RT-PCR results showed significant upregulation of hepatic progenitor cell markers (CK19, SOX9, EpCAM) in the CS group compared to the NC group, as well as in the CSDEN group compared to the DEN group. Our study suggests that *C. sinensis* infection increases risk of HCC in a rat model by stimulating proliferation of hepatic progenitor cells.

Keywords *Clonorchis sinensis* · Hepatocellular carcinoma · Hepatic progenitor cell · Diethylnitrosamine · Cirrhosis

Introduction

Clonorchis sinensis infection (clonorchiasis), induced by the consumption of infected raw freshwater fish, is a foodborne trematodiasis that is predominantly endemic in Asian countries including China, Korea, Japan, and Vietnam (Na et al. 2020). Approximately 35 million people are infected by *C. sinensis*, of whom approximately 14.8 million are in China every year(Qian et al. 2016). Epidemiological evidence and studies in animal models(Prueksapanich et al. 2018) have identified *C. sinensis* as a risk factor for cholangiocarcinoma, and in 2009 it was classified as a group 1 carcinogen by the International Agency for Research on Cancer(Bouvard et al. 2009).

Hepatocellular carcinoma (HCC) was the sixth most commonly diagnosed cancer and the fourth leading cause of cancer death worldwide in 2018, and about 841,000 new cases and 782,000 deaths are reported per year. Half of new cases occur in China, with the main risk factors including chronic hepatitis B virus (HBV) infection, heavy alcohol consumption, obesity, smoking, and exposure to aflatoxin(Bray et al. 2018; Villanueva 2019). Epidemiological and clinical studies have detected clonorchiasis in more than 10% of HCC patients in areas of China where the trematode is endemic(TanTan et al. 2008). In 2015, a

Section Editor: David Bruce Conn

✉ Bangde Xiang
xiangbangde@gxmu.edu.cn

[1] Department of Hepatobiliary Surgery, Guangxi Medical University Cancer Hospital, Nanning 530021, China

[2] Division of Health Science, Graduate School of Health Science, Suzuka University of Medical Science, Mie 5100293, Japan

[3] Key Laboratory of Early Prevention and Treatment for Regional High Frequency Tumors, Ministry of Education, Nanning 530021, China

meta-analysis shows significant associations were found between *C. sinensis* infection hepatocellular carcinoma (OR 4.69, $P < 0.001$) and that more severe infection was associated with higher incidence(Xia et al. 2015). This raises the question of whether and how clonorchiasis may contribute to risk of HCC.

To address this question, we employed a rat model of HCC in which animals were treated with diethylnitrosamine (DEN).

Materials and methods

Preparation of C. sinensis metacercariae

C. sinensis metacercariae were isolated from freshwater fish (*Pseudorasbora parva*) from a freshwater lake in Hengxian County, Guangxi, China. The metacercariae were digested with an acidic pepsin solution (1% HCl, 0.6% pepsin, pH 2.0) to remove the cyst wall and release the infectious worms, which were collected under a stereomicroscope.

Experimental animals

A total of 110 4–6 weeks Sprague–Dawley rats weighing 180–200 g were purchased from the Animal Experiment Center of Guangxi Medical University. The rats were maintained in a specific pathogen-free room on a 12-h light/dark cycle. The rats were housed at four animals per cage, and they were allowed standard chow and water ad libitum. All the rats were fed adaptively for 1 week, then randomly divided into four groups as described below.

Experimental design

Animals were divided into four groups: a negative control (NC) group ($n = 20$), a group infected with *C. sinensis* (CS, $n = 20$), a group with DEN-induced HCC (DEN, $n = 30$), and a group with DEN-induced HCC and *C. sinensis* infection (CSDEN, $n = 40$). The experimental design is shown in Fig. 1. Briefly, each rat in the CS group and the CSDEN group was infected with 150 metacercariae by single intragastric administration at the beginning of the experiment, while the rats in the NC and DEN groups received saline. The animals in the DEN and CSDEN groups received a single intraperitoneal injection of 50 mg/kg DEN (Sigma, St. Louis, MO, USA) at 4 weeks after CS infection(Moreira et al. 2017).

At 10 and 16 weeks after CS or control treatment, 4–8 rats in each group were randomly chosen and euthanized. All remaining rats were euthanized at 22 weeks after the beginning of the experiment.

The animal protocol was reviewed and approved by the Animal Ethics Committee of Guangxi Medical University. All experiments were conducted following the guidelines of the National Standard GB/T35892-2018 of the People's Republic of China. Efforts were made to minimize the suffering of rats: DEN was applied in a relatively low dose, and animals were euthanized with diethyl ether. The

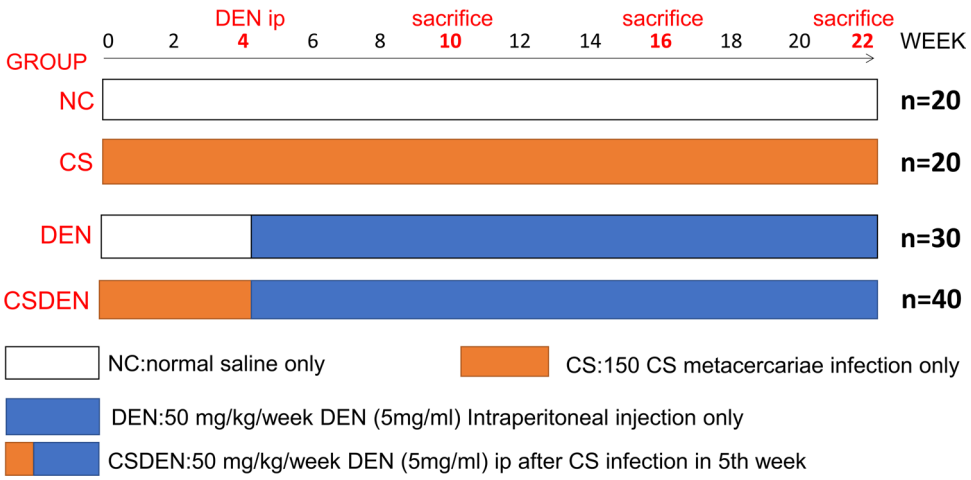

Fig. 1 Study design. A total of 110 Sprague–Dawley rats were divided into four treatment groups. The negative control group (NC) received intragastric administration of saline at the beginning of the experiment (week 0). The clonorchiasis group (CS) received intragastric administration of 150 *C. sinensis* metacercariae at week 0. The diethylnitrosamine-induced group (DEN) received intragastric administration of saline on week 0, followed by intraperitoneal administration of DEN on week 4. The clonorchiasis diethylnitrosamine-induced group (CSDEN) received intragastric administration of 150 *C. sinensis* metacercariae at week 0, followed by intraperitoneal administration of DEN on week 4. At weeks 10 and 16, 4–8 animals from each group were sacrificed and tissues isolated. All remaining animals were sacrificed at week 22

number of animals was minimized in accordance with the guidelines of our institutional Animal Ethics Committee.

Gene expression analysis

The expression of keratin-19 (CK19), sex-determining region *Y* box protein 9 (SOX9), and epithelial cell adhesion molecule (EpCAM) in liver was investigated using real-time PCR. β-actin was used as an endogenous control. Primers were designed based on GenBank sequences as shown in Table 1. Total RNA was extracted from hepatic parenchyma (NC and CS groups) or from hepatic tissue (DEN and CSDEN groups) using TRIZOL (Invitrogen, Carlsbad, CA, USA). The expression levels of CK19, SOX9, and EPCAM were determined by reverse transcription and real-time PCR using an SYBR Premix Ex Taq Kit and Thermal Cycler Dice Real-Time System (TAKARA BIO, Ootsu, Shiga, Japan) according to the manufacturer's instructions. PCR amplification was performed under the following conditions: 1 cycle pre-denaturation at 95℃ for 10 s, 40 cycles of amplification at 95℃ for 5 s and 60℃ for 30 s. Melting curve analysis was performed from 60 to 95℃ in heating steps of 0.1℃/s.

RNA sequencing

Total RNA was extracted as described above from 10^6 cells. The integrity of the isolated RNA was determined using a 2100 Bioanalyzer (Agilent) and quantified using a NanoDrop system (Thermo Scientific). About 1 μg of high-quality RNA was used to construct the sequencing library. RNA purification, reverse transcription, library construction, and sequencing were performed at WuXi NextCODE (Shanghai, China) on an Illumina platform according to the manufacturer's instructions.

Table 1 Sequences of primers used for RT-PCR

Primer	Sequence (5' to 3')	Nt
CK19-F	AGTCTTCTCAGCCAAACCCTC	21
CK19-R	CTGGTCTGTGGAACTAGGCA	20
SOX9-F	ACCCACCACTCCCAAAACAG	20
SOX9-R	CGGCAGGTATTGGTCAAACTC	21
EpCAM-F	CATTGTCGTGGTGGTGTTAGC	21
EpCAM-R	CCCATCTCCTTTATCTCAGCC	21
IL6-F	TGCCTTCTTGGGACTGATGT	20
IL6-R	ATACTGGTCTGTTGTGGGTG	20
actin-F	TATCCTGGCCTCACTGTCCA	20
actin-R	AAGGGTGTAAAACGCAGCTCA	21

Histopathology

The liver tissue was carefully collected after euthanasia and fixed in 10% buffered formalin. Specimens were conventionally processed for histology, and sections were stained with hematoxylin and eosin (H&E), Masson's trichrome stain, or immunohistochemical reagents. The liver sections were analyzed under an inverted microscope (Nikon ECLIPSE Ti, Tokyo, Japan). Degree of fibrosis was scored as follows: 0 = no fibrosis; 1 = central venous or portal area around mild fibrosis; 2 = short fibrous interval between the central veins; 3 = long fibrous interval not completely separated from the hepatic lobule; 4 = early stage liver fibrosis involving a large pseudolobule and frequent square-shaped portal areas; 5 = cirrhosis of the liver, nodules of various size mixed together, small nodules less than 50%; 6 = cirrhosis of the liver, mainly small nodules with fibrous, widened septa.

Immunohistochemical stainings were scored as follows: 0 = no or small positive staining area (< 10%), 1 = positive staining area < 30%, 2 = positive staining area 30–60%, 3 = positive staining area > 60%.

Statistical analysis

All analyses were performed using SPSS 19.0 (IBM, Chicago, USA). Continuous data were expressed as mean ± SD. Inter-group differences were assessed for significance using Student's *t*-test in the case of continuous variables, or the Mann–Whitney *U* test in the case of non-parametric variables. Differences in categorical variables were assessed using the chi-squared test or Fisher's exact test. Differences associated with $P < 0.05$ were considered statistically significant.

Results

Confirmation of C. sinensis infection in rats

To ascertain successful infection of the animals, we inspected animal feces for the presence of *C. sinensis* eggs. At 4 weeks after infection, eggs were found in the stool of 81.7% of rats in the CS and CSDEN groups, with no eggs observed in the NC or DEN groups (Fig. 2). Only CS-infected animals were used in CS or CSDEN groups this experiment. Two rats in the DEN group and five rats in the CSDEN group died between weeks 18 and 22 because of hemoperitoneum, hepatic failure, or liver rupture, and these seven rats were excluded from analysis.

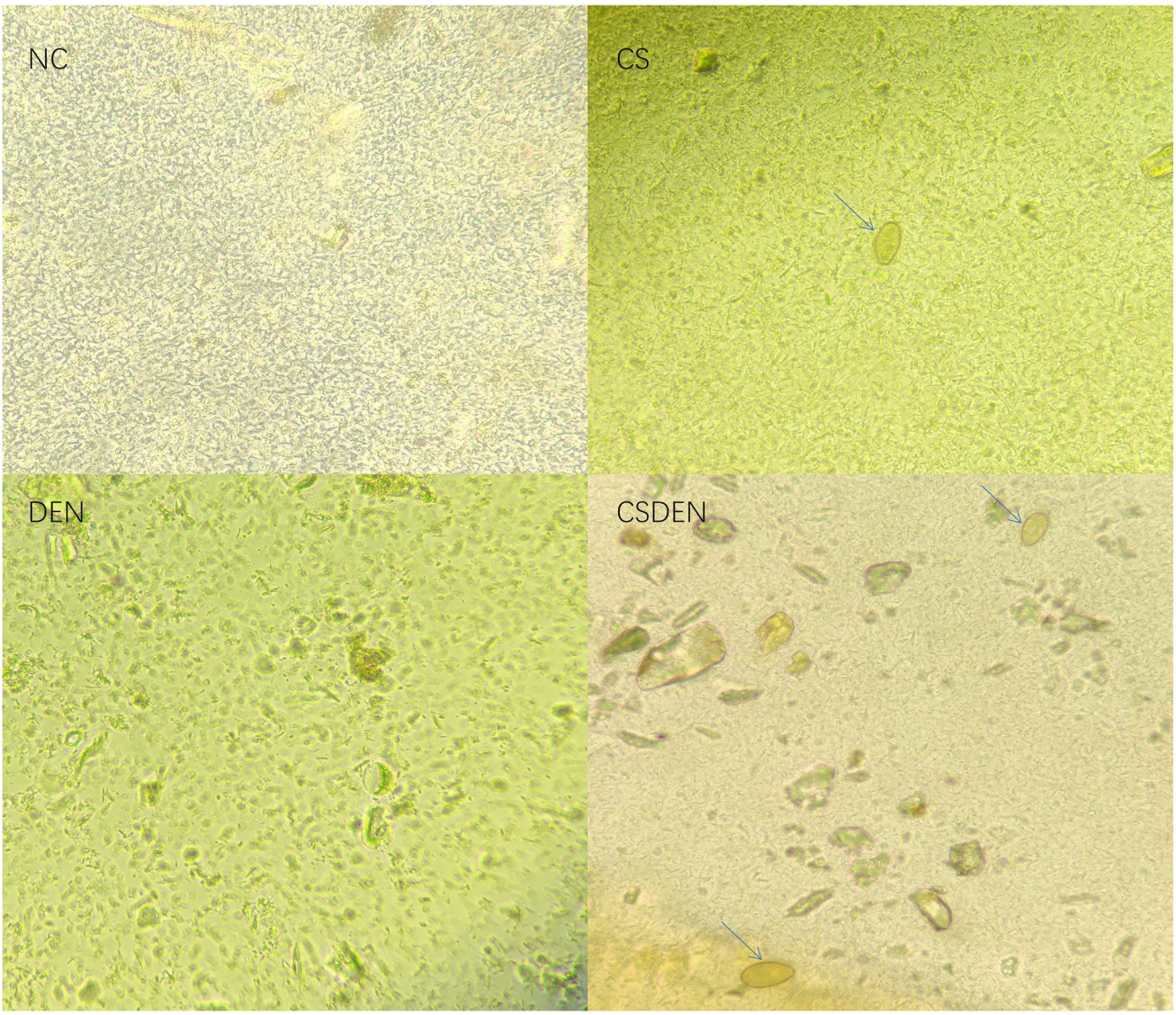

Fig. 2 Confirmation of *C. sinensis* infection. Detection of eggs in the feces of rats at week 4 post-infection. Images from one representative animal per treatment are shown. The blue arrow indicates *C. sinensis* eggs. Magnification: 4 × 10

Gross examination of rat liver after infection

We next analyzed the liver in all groups (Fig. 3). In the NC group, the liver had a soft, smooth surface without abnormal lesions. In the CS group, the liver was dark red, and it appeared slightly larger and heavier than in the NC group. Most importantly, the bile duct was significantly dilated and contained many adult worms. In the DEN group, the liver had a rough surface without nodules at week 10, with no abnormalities in the bile duct. The liver in three of eight rats showed development of liver cirrhosis at week 16. The liver of 15 rats was enlarged, and surface tumor nodules were observed in two rats at week 22. In the CSDEN group, the liver surface had a hard rough texture without abnormal lesions, and many adult worms were found in the dilated bile ducts at weeks 10 and 16. Surface tumor nodules were seen on the liver of five rats at week 22.

Histopathology of rat liver after infection

No pathological changes were observed in the NC group. In the CS group, a dilated bile duct containing adult worms was found, and many eggs were observed in the worms. One of the most obvious abnormalities in this group was a large number of proliferating biliary epithelial cells with hyperchromatic cholangiocyte nuclei surrounding the worms, with goblet cells occasionally found between biliary epithelial cells. Additionally, many bile ducts exhibited adenomatous hyperplasia, periportal fibrosis, or periductal fibrosis in their

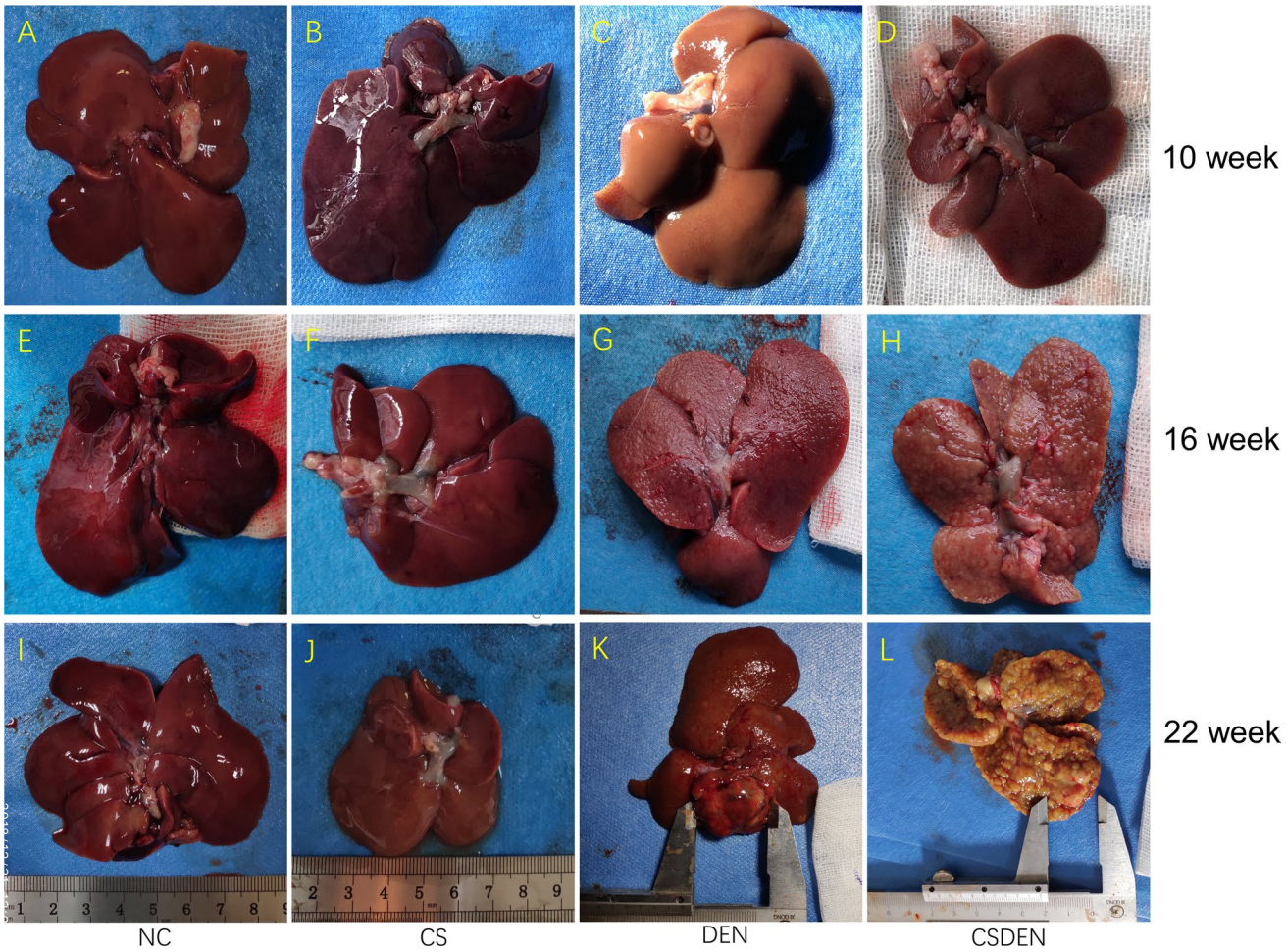

Fig. 3 Gross examination of liver after infection. Gross pathology of the liver of rats sacrificed at weeks 10, 16, and 22 after infection. An image from one representative animal is shown per panel

central sections. The presence of lymphocytes, monocytes, and eosinophils indicated an inflammatory response.

In the DEN group, the results of H&E staining of the liver at weeks 10 and 16 showed enlargement of some hepatocytes due to edema, necrosis of some hepatocytes, fibroplasia, and infiltration of inflammatory cells such as lymphocytes in the portal area. At week 22, 15 rats were still alive, of which nine exhibited liver cirrhosis and seven exhibited HCC.

In the CSDEN group, adenomatous hyperplasia, periportal fibrosis, and periductal fibrosis were observed at the beginning of the experiment, and infiltration of inflammatory cells including lymphocytes, monocyte, and eosinophils was observed in the portal area. At week 22, the most distinctive abnormality was a large number of proliferating bile ducts that had invaded the liver parenchyma, leading to obvious ductular reactions. Hepatocytes were generally edematous and degenerated, and hepatocyte steatosis was observed. Many tumor cells were found in the liver of all 17 rats (Fig. 4).

H&E and immunohistochemical staining for the tumor marker cytokeratin 19 indicated that 15 of 17 rats had HCC, while only 2 rats had cholangiocarcinoma (CCA). One animal showed both HCC and CCA. The HCC formation rate in the CSDEN group was 88.2%, significantly higher than in the DEN group (46.7%, $P = 0.021$; Fig. 5).

Masson staining of rat liver after infection

We next performed Masson staining on rat tissues to evaluate the collagen content (Fig. 6). While no pathological changes were observed in the NC group, there was significant collagen fiber accumulation around the bile duct in the CS group, giving rise to periductal fibrosis. At 10 weeks, grade 1 fibrosis was predominant in the DEN group, while grades 2 and 3 were predominant in the CSDEN group. The severity of periductal fibrosis in the CS group was higher at week 16 than at week 10. At week 22, cirrhosis formation was observed in 3 of 8 rats in the DEN group, while cirrhosis

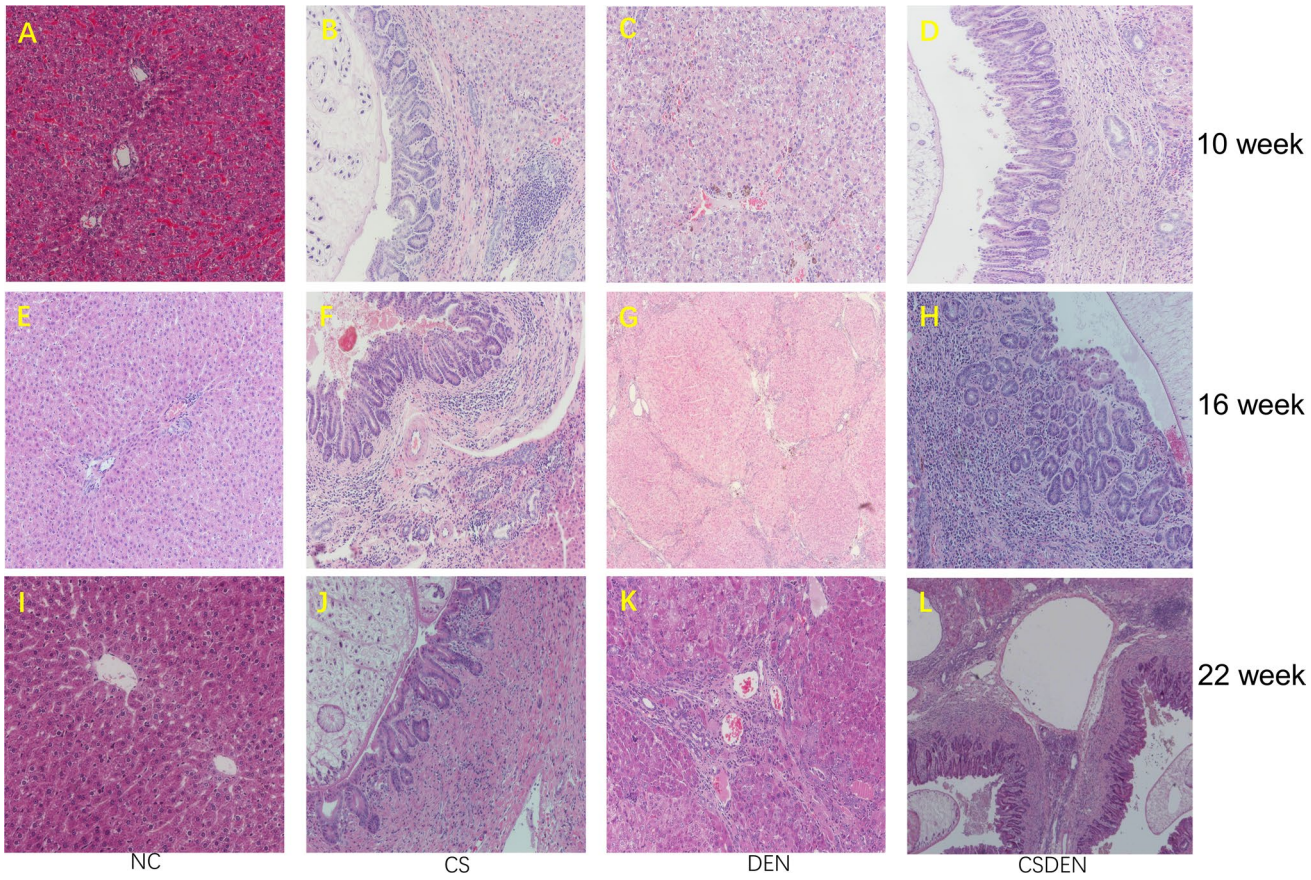

Fig. 4 Histopathogical examination of liver tissue after infection. Histopathological features of liver of rats sacrificed at weeks 10, 16, and 22 after infection. An image from one representative animal is shown per panel. Magnification: 10 × 10

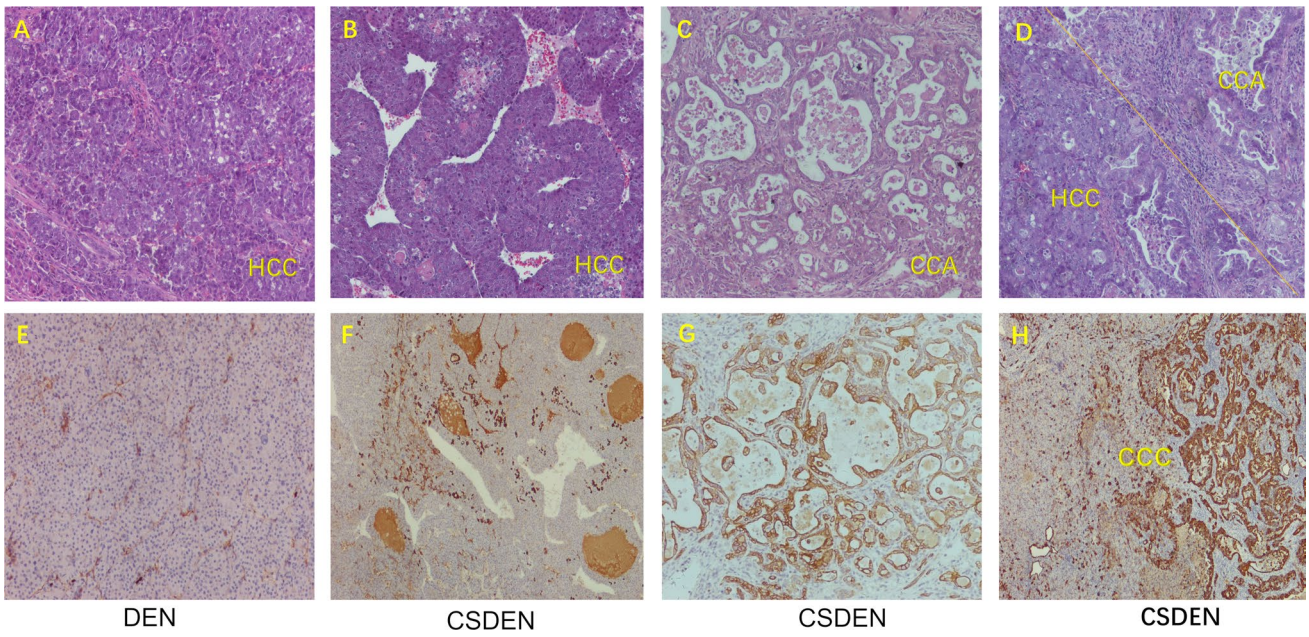

Fig. 5 Histopathological examination of cancerous liver tissue after infection. Histopathological features of the liver of rats sacrificed at week 22 after infection. Representative H&E staining is shown in panels **A**, **B**, **C**, **D**, and representative immunohistochemical staining for cytokeratin 19 is shown in panels **E**, **F**, **G**, **H**. Magnification: 20 × 10

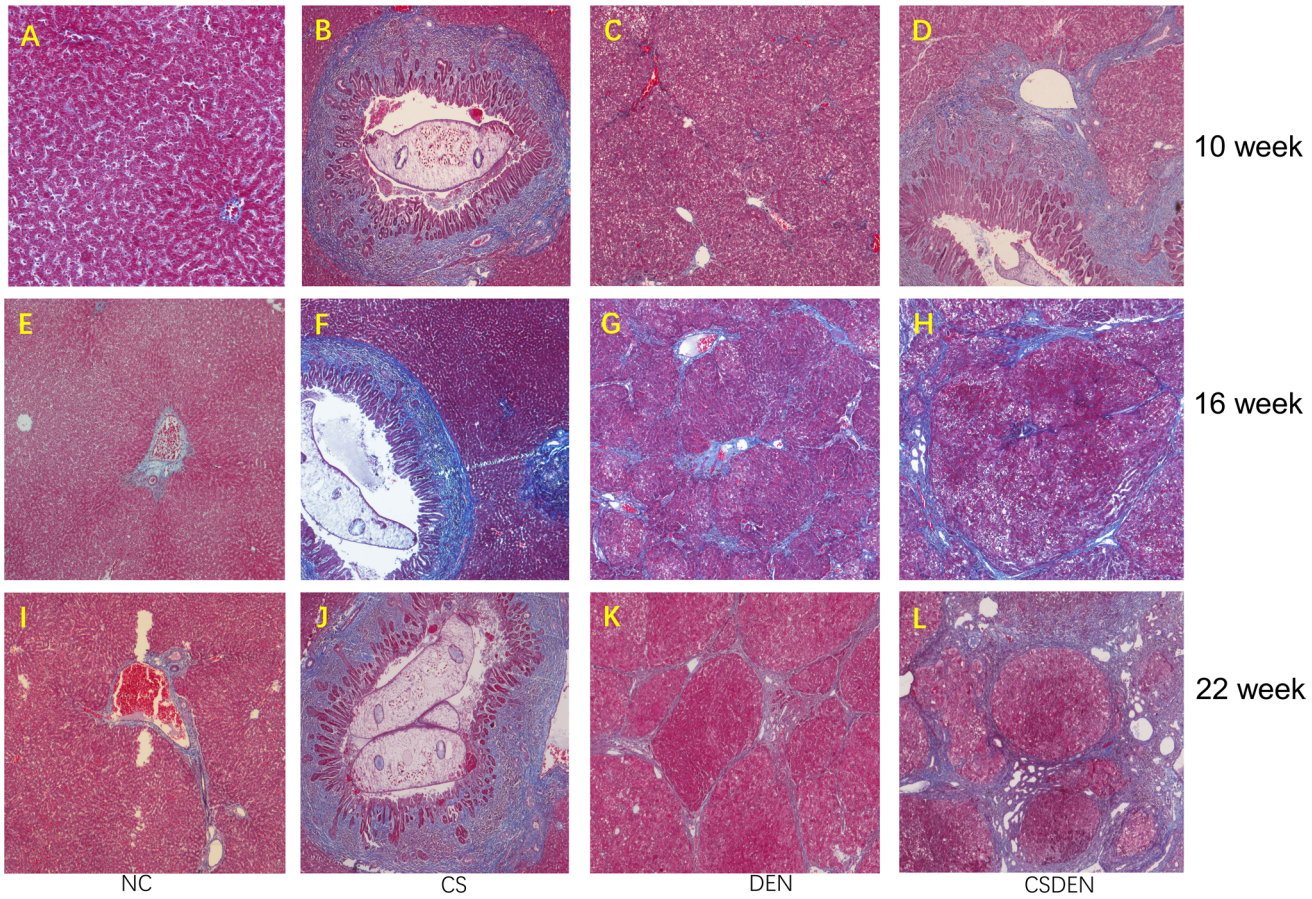

Fig. 6 Collagen staining of liver tissue after infection. Masson's staining of liver tissues of rats sacrificed at weeks 10, 16, and 22 after infection. An image from one representative animal is shown per panel. Magnification: 10 × 10

formation was observed in 5 of 7 rats in the CSDEN group. The incidence of cirrhosis was much higher in the CSDEN group ($n = 17$) than in the DEN group ($n = 9$, $P = 0.006$).

Analysis of differentially expressed genes after infection

To begin to identify the molecular pathways through which infection may increase risk of HCC, we compared the transcriptomes across the different animal groups. We performed RNA-seq on three paired liver tissue samples from the NC and CS groups as well as three paired HCC tissue samples from the DEN and CSDEN groups. All samples were collected at week 22. We screened the sequencing results for differentially expressed genes (DEGs) (cut off: log2foldchange > 1, $P < 0.05$). A total of 253 DEGs were identified between the CS and NC groups, including 118 upregulated and 135 downregulated genes. A total of 7348 DEGs were identified between the DEN and NC groups, including 3518 upregulated and 3830 downregulated genes. A total of 7356 DEGs were identified between the CSDEN and NC groups, including 4485 upregulated and 2871 downregulated genes. Finally, 7322 DEGs were identified between the CSDEN and DEN groups, including 2764 upregulated and 4558 downregulated genes.

We next analyzed DEGs to detect enrichment in Kyoto Encyclopedia of Genes and Genomes (KEGG) pathways. This enrichment analysis was conducted for the following pairwise comparisons: (1) CS vs. NC groups, (2) CSDEN vs. NC groups, and (3) CSDEN vs. DEN groups. In the comparison between CS and NC groups, the significantly upregulated DEGs in the CS group were enriched in the following pathways: hematopoietic cell lineage, complement and coagulation cascades, TNF signaling, breast cancer, mucin type O-glycan biosynthesis, carbohydrate digestion and absorption, signaling involving vascular endothelial growth factor (VEGF), regulation of lipolysis in adipocytes, prolactin signaling, and B-cell receptor signaling (Fig. 7A). The significantly downregulated DEGs in the CS group were enriched in FoxO signaling, TGF-beta signaling, tyrosine metabolism, regulation of lipolysis in adipocytes, synaptic vesicle cycling, and signaling involving PPAR (Fig. 7B).

In the comparison between CSDEN and NC groups, the significantly upregulated DEGs in the CSDEN group

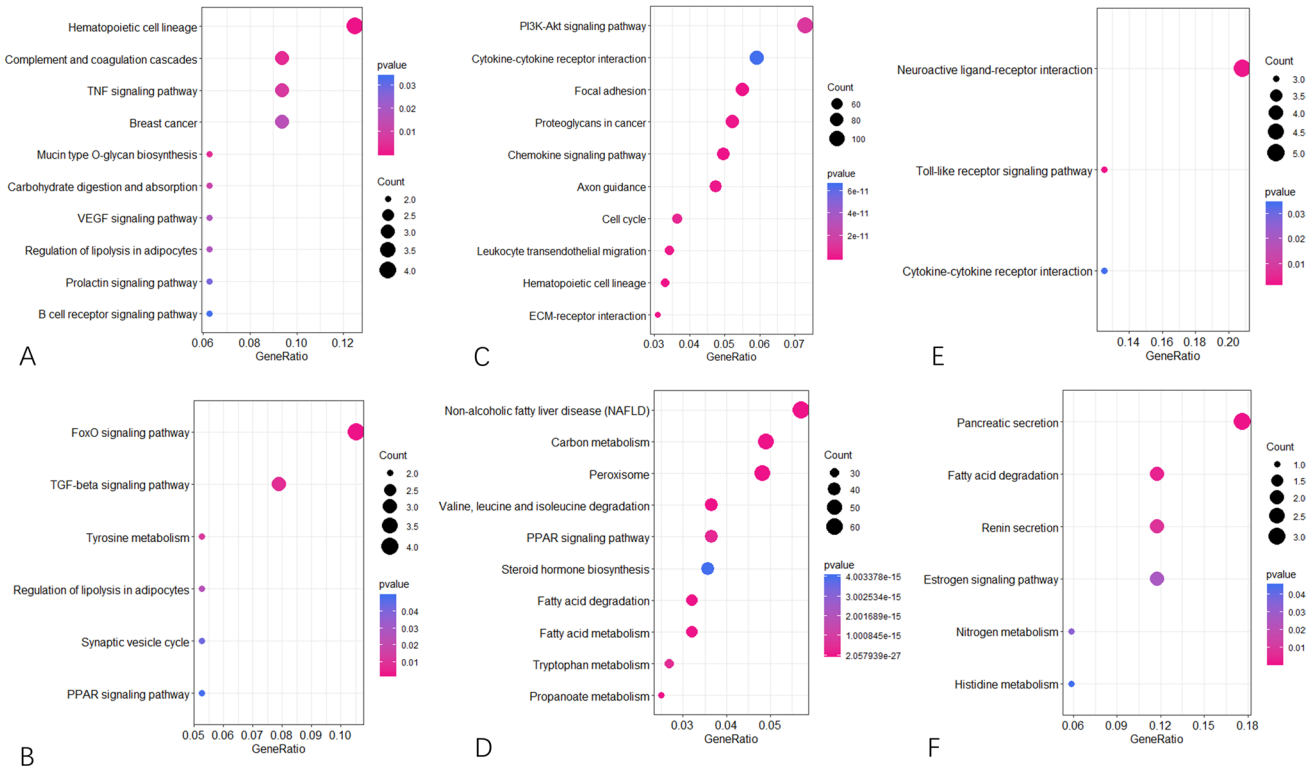

Fig. 7 KEGG enrichment analysis of genes differentially expressed after infection. Pathways enriched in significantly upregulated genes (**A**, **C**, **E**) or significantly downregulated genes (**B**, **D**, **F**) in mouse tissues from the indicated comparisons

were enriched in the following pathways: signaling involving PI3K-Akt, cytokine-cytokine receptor interaction, focal adhesion, proteoglycans in cancer, chemokine signaling, axon guidance, cell cycle, leukocyte transendothelial migration, hematopoietic cell lineage, interactions between receptors, and the extracellular matrix (ECM) (Fig. 7C). The significantly downregulated DEGs were enriched in non-alcoholic fatty liver disease, carbon metabolism, peroxisome, valine, leucine and isoleucine degradation, PPAR signaling, steroid hormone biosynthesis, fatty acid degradation, fatty acid metabolism, tryptophan metabolism, and propanoate metabolism (Fig. 7D).

In the comparison between CSDEN and DEN groups, the significantly upregulated DEGs in the CSDEN group were enriched in the following pathways: neuroactive ligand-receptor interaction, Toll-like receptor signaling, and cytokine-cytokine receptor interaction (Fig. 7E). The significantly downregulated DEGs were enriched in pancreatic secretion, fatty acid degradation, renin secretion, estrogen signaling pathway, nitrogen metabolism, and histidine metabolism (Fig. 7F).

C. sinensis promotes HCC by activating hepatic progenitor cells

Hepatic progenitor cells (HPCs) are hepatic stem cells, which are defined as bipotential cells that can differentiate into both hepatocytes and cholangiocytes. We hypothesized that *C. sinensis* promotes HCC by activating HPCs. Therefore, we evaluated the expression of the HPC markers CK19, SOX9, and EpCAM in all our rat groups. Strong CK19 expression was observed mainly in the CS and CSDEN groups, with low expression in the liver tissues of NC and DEN groups. CK19 was highly expressed in proliferating cholangiocytes in the CS group. CK19 was found not only in cholangiocytes but also in hepatocytes in the center of hepatic lobules at weeks 16 and 22 in the CSDEN group. CK19 was not expressed in hepatocytes in the NC or CS groups, which may indicate that CS and DEN synergistically trigger the malignant transformation of HPCs to HCC cells (Fig. 8).

SOX9, which is located mainly in the nucleus(Rizvi et al. 2017), was rarely expressed in liver tissues of the NC group,

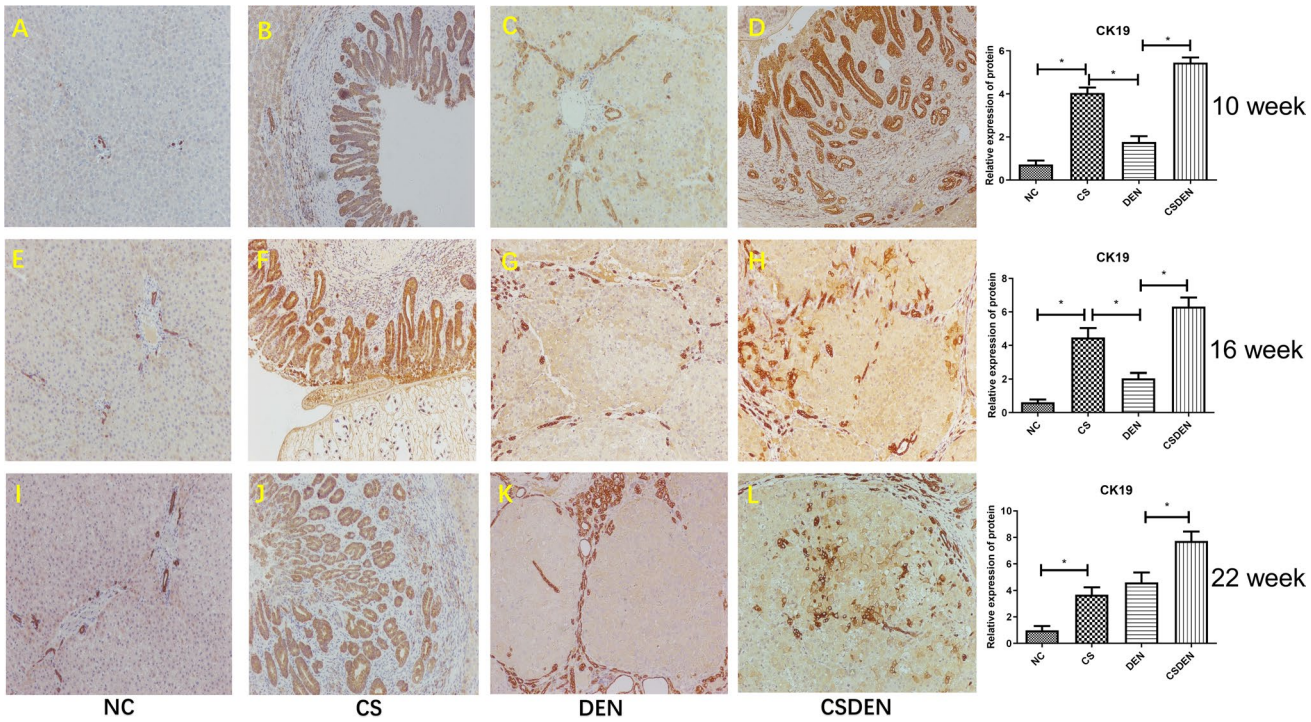

Fig. 8 CK19 expression in the liver after infection. Immunohistochemical staining for cytokeratin 19 (CK19) in liver of rats sacrificed at weeks 10, 16, and 22 after infection. An image from one representative animal is shown per panel. Relative quantification at each time point is shown on the far right. $*P < 0.05$. Magnification: 20 × 10

but it was upregulated in the liver of the CS group, particularly in CS-induced proliferating cholangiocytes. The liver showed high SOX9 expression the DEN and CSDEN groups, higher than in the DEN group. At week 10, SOX9 was expressed mostly in cholangiocytes and less in hepatocytes, but the expression in hepatocytes increased with time. At weeks 16 and 22, SOX9 expression in hepatocytes of the CSDEN group increased above the level in the DEN group (Fig. 9).

The expression of EpCAM, which localizes mainly on the cell membrane(Xie et al. 2005), partially mimicked that of SOX9 and CK19. In the NC and CS groups, EpCAM was detected only in cholangiocytes and not in hepatocytes. Its expression in proliferating cholangiocytes was higher in the CS group. EpCAM was expressed at higher levels in the DEN and especially CSDEN groups than in the NC and CS groups. Unlike SOX9 and CK19, EpCAM was detectable in hepatocytes of the CSDEN group at week 16 and in hepatocytes of the DEN group at week 22 (Fig. 10).

These immunohistochemical results collectively show that the expression of CK19, SOX9, and EpCAM in hepatocytes generally increased with the duration of *C. sinensis* infection. We confirmed this time-dependent upregulation at the mRNA level, which also confirmed that expression of all three markers was higher in the CS group than in the NC group, and higher in the CSDEN group than in the DEN group (Fig. 11).

We interpret the increased expression of HCC markers to indicate CS-induced activation of HPCs, which may promote HCC development.

Discussion

Our study demonstrates that *C. sinensis* can contribute to the development of HCC by accelerating tumor formation. This would explain the much higher incidence of cirrhosis and HCC in the CSDEN group than in the DEN group. Our work provides rigorous confirmation of earlier work that showed that treating Syrian golden hamsters with DEN and *C. sinensis* led to higher rates of HCC and CCA than treating them with DEN alone. Even earlier work showed in an animal model that the trematode *Opisthorchis viverrini*-induced precancerous hepatocellular nodules and CCA (Thamavit et al. 1987, 1988).

In our study, the livers of rats infected with *C. sinensis* developed only papillary or adenomatous hyperplasia and inflammatory infiltration, but not HCC or CCA, which is consistent with previous studies(Zheng et al. 2017) and may reflect the short infection of 22 weeks. Studies showing that

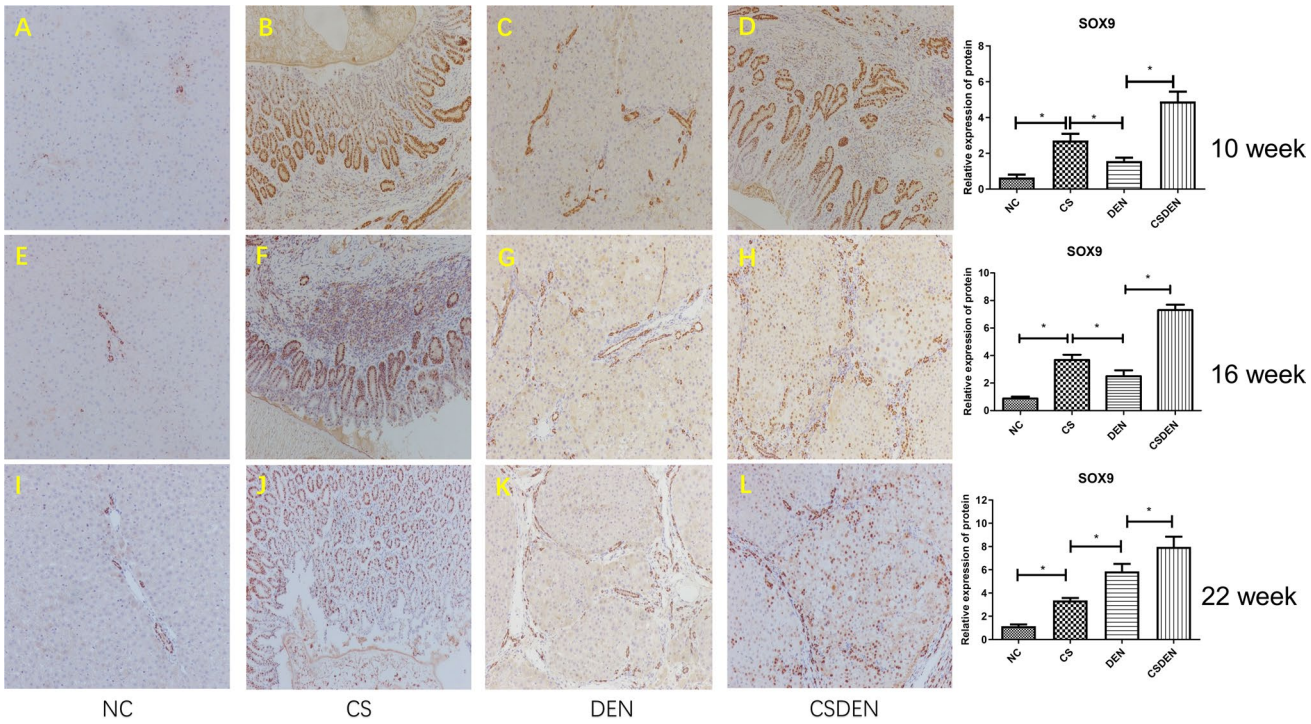

Fig. 9 SOX9 expression in the liver after infection. Immunohistochemical staining for sex-determining region *Y* box protein 9 (SOX9) in liver of rats sacrificed at weeks 10, 16, and 22 after infection. An image from one representative animal is shown per panel. Relative quantification at each time point is shown on the far right. Magnification: 20 × 10.*$P < 0.05$

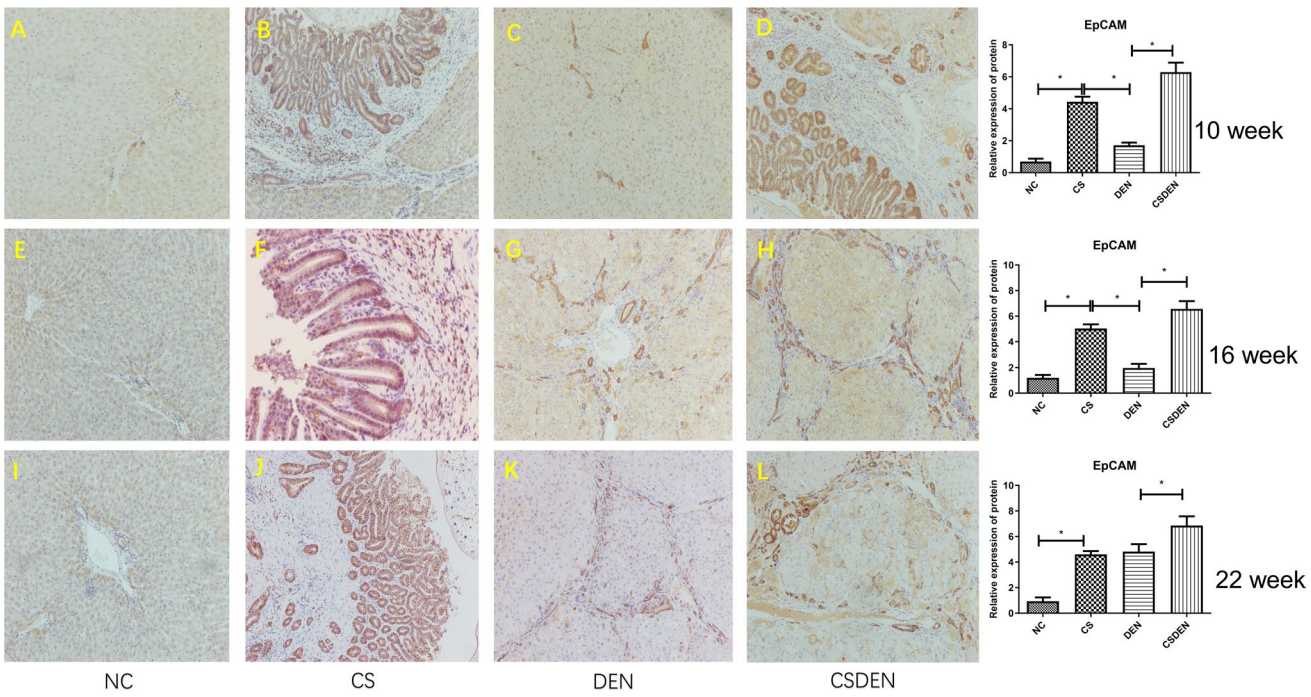

Fig. 10 EpCAM expression in the liver after infection. Immunohistochemical staining for epithelial cell adhesion molecule (EpCAM) protein in liver of rats sacrificed at weeks 10, 16, and 22 after infection. An image from one representative animal is shown per panel. Relative quantification at each time point is shown on the far right. Magnification: 20 × 10. *$P < 0.05$

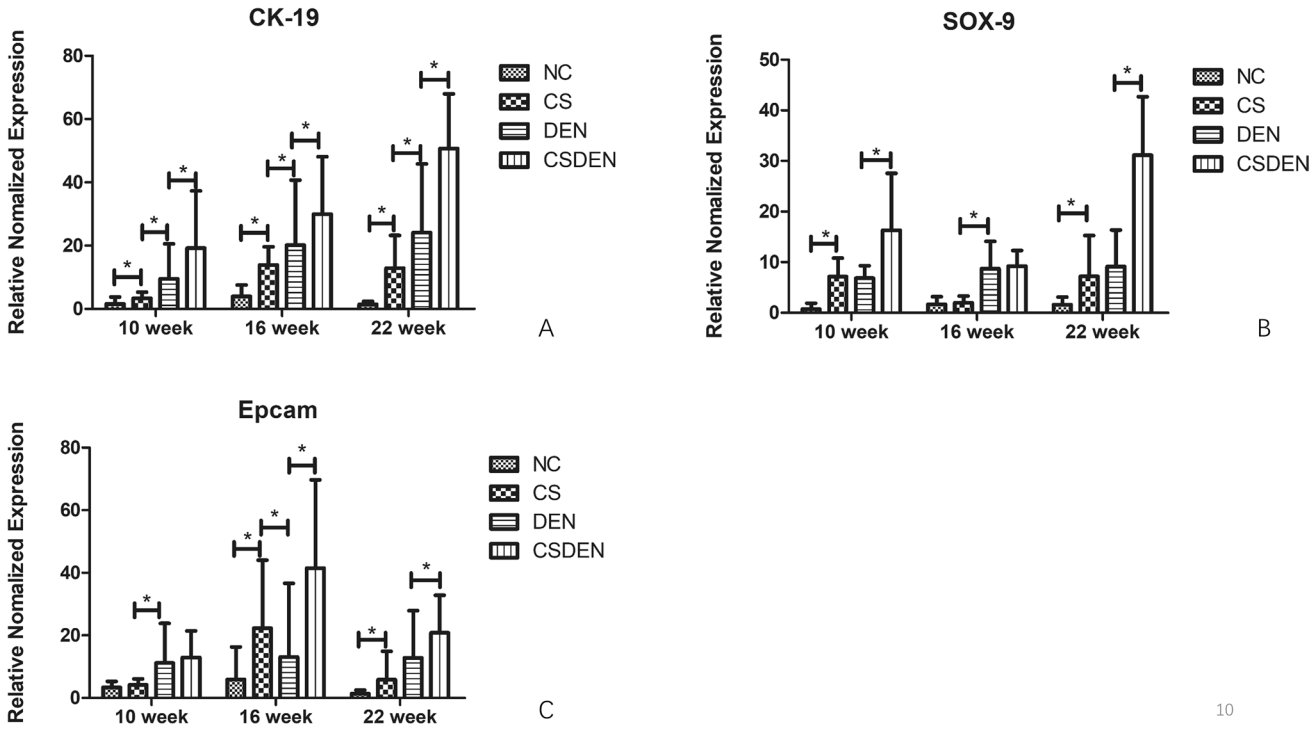

Fig. 11 Relative expression of biomarkers of hepatic progenitor cells. The relative mRNA levels of CK19, SOX9, and EpCAM in liver of rats sacrificed at weeks 10, 16, and 22 after infection, as determined by RT-PCR. $*P < 0.05$

O. viverrini can induce CCA examined infections lasting up to 20 months (Songserm et al. 2009).

We observed more severe fibrosis in the CSDEN group than in the DEN group, consistent with studies indicating that *C. sinensis*-induced immune-inflammatory responses and *C. sinensis*-secreted factors can cause liver fibrosis (Yan et al. 2017). Indeed, we observed extensive fibrosis around the bile duct and cirrhosis of *C. sinensis*-infected rats, suggesting that *C. sinensis* can directly induce liver fibrosis. Long-term fibrosis, in turn, increases risk of cirrhosis and even HCC.

We observed several factors that led us to implicate HPCs in the pathology of the CSDEN group. Those animals showed a strong ductular reaction, which is thought to be mediated by HPCs (Williams et al. 2014). Indeed, we observed strong upregulation of CK19, SOX9, and EpCAM relative to both the NC and DEN groups. In fact, we observed upregulation also in the CS group relative to the NC group. HPCs have been linked to HCC, CCA, and combined hepatocellular cholangiocarcinoma(Zhao et al. 2016; Komuta et al. 2008; Sia et al. 2017). Inflammation appears to contribute to several types of cancer, including HCC (Diakos et al. 2014). For example, chronic inflammation activates the proliferation of HPCs and differentiation into HCC stem cells, which can cause HCC (Li et al. 2017). Therefore, we propose that *C. sinensis* induces chronic inflammation that activates the malignant transformation of HPCs and hepatic stem cells.

In support of our hypothesis, our RNA-seq analysis suggests that the DEGs in the CSDEN group are involved in Toll-like receptor signaling, which is a classic inflammation-associated pathway. *C. sinensis* secretes the protein ESP, which activates Toll-like receptors 1 and 4 on the membrane of inflammatory cells. Constitutive activation of this signaling pathway can initiate chronic inflammation (Bahk and Pak 2016). Although *C. sinensis* has conventionally been thought to promote CCA primarily, our animal study indicates that it can also contribute to HCC. In fact, our data suggest that the pathogen can give rise to either of these diseases or to combined hepatocellular cholangiocarcinoma by creating a chronically inflammatory microenvironment within the liver, which activates HPCs to differentiate into liver stem cells.

Other classical signaling pathways related to inflammation have been found in our study, such as TNF signaling(Giosia et al. 2022) and PI3K-Akt signaling(Zhao et al. 2021). Our study shows chronic inflammatory is triggered and sustained by *C. sinensis* infection and chronic inflammation is a potent driving force in HCC tumorigenesis, The activation of these inflammation-related signaling pathways over time lead to overproduction of reactive oxygen species (ROS) and reactive nitrogen species, all of the

above can leads to activation of HPCs, and easily lead to the occurrence of HCC(Llovet et al. 2022).

An important shortcoming of our study is that most patients with HCC in China also have chronic HBV infection (Yip et al. 2020), which we did not take into account in our animal experiments and so should be explored in future studies. Nevertheless, our findings justify further work on the role of *C. sinensis* in HCC. Such work may contribute not only to the management and control of *C. sinensis*, but also to efforts to reduce HCC incidence.

Author contribution Bangde Xiang: obtained funding; conceived and designed the study, Yapeng Qi: analyzed the data and drafted the first version of the manuscript. Junwen Hu, Jiahao Liang Xiaoyin Hu: acquisition of data; analysis and interpretation of data. Ning Ma: material support; critical revision of the manuscript for important intellectual content; study supervision. All authors read and approved the final manuscript.

Funding This work was supported by grants from the National Natural Science Foundation of China (81960450), National Major Special Science and Technology Project (2017ZX10203207), High-level Innovation Team and Outstanding Scholar Program of Guangxi Colleges and Universities,"139" Projects for Training of High-level Medical Science Talents from Guangxi, Key Research and Development Project of Guangxi (AA18221001, AB18050020, 2020AB34006), Key Laboratory of Early Prevention and Treatment for Regional High Frequency Tumors, Ministry of Education of Guangxi, Independent Research Projects (GKE2017-ZZ02, GKE2018-KF02, GKE2019-ZZ07), and Development and Application of Medical and Health-appropriate Technology in Guangxi (S2019039).

Declarations

Conflict of interest The authors declare no competing interests.

References

Bahk YY, Pak JH (2016) Toll-like receptor-mediated free radical generation in *Clonorchissinensis* excretory-secretory product-treated cholangiocarcinoma cells. The Korean J Parasitol 54(5):679–684. https://doi.org/10.3347/kjp.2016.54.5.679

Bouvard V, Baan R, Straif K, Grosse Y, Secretan B, El Ghissassi F, Benbrahim-Tallaa L, Guha N, Freeman C, Galichet L, Cogliano V, WHO International Agency for Research on Cancer Monograph Working Group (2009) A review of human carcinogens–Part B: biological agents. The Lancet Oncol 10(4):321–322. https://doi.org/10.1016/s1470-2045(09)70096-8

Bray F, Ferlay J, Soerjomataram I, Siegel RL, Torre LA, Jemal A (2018) Global cancer statistics 2018: GLOBOCAN estimates of incidence and mortality worldwide for 36 cancers in 185 countries. CA: A Cancer J Clin 68(6):394–424. https://doi.org/10.3322/caac.21492

Di Giosia P, Stamerra CA, Giorgini P, Jamialahamdi T, Butler AE, Sahebkar A (2022) The role of nutrition in inflammaging. Ageing Res Rev 77:101596. https://doi.org/10.1016/j.arr.2022.101596

Diakos CI, Charles KA, McMillan DC, Clarke SJ (2014) Cancer-related inflammation and treatment effectiveness. The Lancet Oncol 15(11):e493–e503. https://doi.org/10.1016/S1470-2045(14)70263-3

Komuta M, Spee B, Vander Borght S, De Vos R, Verslype C, Aerts R, Yano H, Suzuki T, Matsuda M, Fujii H, Desmet VJ, Kojiro M, Roskams T (2008) Clinicopathological study on cholangiolocellular carcinoma suggesting hepatic progenitor cell origin. Hepatol (Baltimore Md) 47(5):1544–1556. https://doi.org/10.1002/hep.22238

Li XF, Chen C, Xiang DM, Qu L, Sun W, Lu XY, Zhou TF, Chen SZ, Ning BF, Cheng Z, Xia MY, Shen WF, Yang W, Wen W, Lee T, Cong WM, Wang HY, Ding J (2017) Chronic inflammation-elicited liver progenitor cell conversion to liver cancer stem cell with clinical significance. Hepatol (Baltimore Md) 66(6):1934–1951. https://doi.org/10.1002/hep.29372

Llovet JM, Castet F, Heikenwalder M, Maini MK, Mazzaferro V, Pinato DJ, Pikarsky E, Zhu AX, Finn RS (2022) Immunotherapies for hepatocellular carcinoma. Nat Rev Clin Oncol 19(3):151–172. https://doi.org/10.1038/s41571-021-00573-2

Moreira AJ, Rodrigues GR, Bona S, Fratta LX, Weber GR, Picada JN, Dos Santos JL, Cerski CT, Marroni CA, Marroni NP (2017) Ductular reaction, cytokeratin 7 positivity, and gamma-glutamyl transferase in multistage hepatocarcinogenesis in rats. Protoplasma 254(2):911–920. https://doi.org/10.1007/s00709-016-1000-0

Na BK, Pak JH, Hong SJ (2020) *Clonorchis sinensis* and clonorchiasis. Acta Trop 203:105309. https://doi.org/10.1016/j.actatropica.2019.105309

Prueksapanich P, Piyachaturawat P, Aumpansub P, Ridtitid W, Chaiteerakij R, Rerknimitr R (2018) Liver fluke-associated biliary tract cancer. Gut and Liver 12(3):236–245. https://doi.org/10.5009/gnl17102

Qian MB, Utzinger J, Keiser J, Zhou XN (2016) Clonorchiasis. Lancet (london, England) 387(10020):800–810. https://doi.org/10.1016/S0140-6736(15)60313-0

Rizvi S, Fischbach SR, Bronk SF, Hirsova P, Krishnan A, Dhanasekaran R, Smadbeck JB, Smoot RL, Vasmatzis G, Gores GJ (2017) YAP-associated chromosomal instability and cholangiocarcinoma in mice. Oncotarget 9(5):5892–5905. https://doi.org/10.18632/oncotarget.23638

Sia D, Villanueva A, Friedman SL, Llovet JM (2017) Liver cancer cell of origin, molecular class, and effects on patient prognosis. Gastroenterology 152(4):745–761. https://doi.org/10.1053/j.gastro.2016.11.048

Songserm N, Prasongwattana J, Sithithaworn P, Sripa B, Pipitkool V (2009) Cholangiocarcinoma in experimental hamsters with long-standing *Opisthorchis viverrini* infection. Asian Pacific J Cancer Prev : APJCP 10(2):299–302

TanTan SK, Qiu XQ, Yu HP, Zeng XY, Zhao YN, Hu L (2008) Evaluation of the risk of clonorchiasis inducing primary hepatocellular carcinoma. Zhonghua Gan Zang Bing Za Zhi 16(2):114–116 (**Chinese**)

Thamavit W, Ngamying M, Boonpucknavig V, Boonpucknavig S, Moore MA (1987) Enhancement of DEN-induced hepatocellular nodule development by *Opisthorchis viverrini* infection in Syrian golden hamsters. Carcinogenesis 8(9):1351–1353. https://doi.org/10.1093/carcin/8.9.1351

Thamavit W, Moore MA, Hiasa Y, Ito N (1988) Enhancement of DHPN induced hepatocellular, cholangiocellular and pancreatic carcinogenesis by *Opisthorchis viverrini* infestation in Syrian golden hamsters. Carcinogenesis 9(6):1095–1098. https://doi.org/10.1093/carcin/9.6.1095

Villanueva A (2019) Hepatocellular carcinoma. N Engl J Med 380(15):1450–1462. https://doi.org/10.1056/NEJMra1713263

Williams MJ, Clouston AD, Forbes SJ (2014) Links between hepatic fibrosis, ductular reaction, and progenitor cell expansion. Gastroenterology 146(2):349–356. https://doi.org/10.1053/j.gastro.2013.11.034

Xia J, Jiang SC, Peng HJ (2015) Association between liver fluke infection and hepatobiliary pathological changes: a systematic review

and meta-analysis. PLoS ONE 10(7):e0132673. https://doi.org/10.1371/journal.pone.0132673

Xie X, Wang CY, Cao YX, Wang W, Zhuang R, Chen LH, Dang NN, Fang L, Jin BQ (2005) Expression pattern of epithelial cell adhesion molecule on normal and malignant colon tissues. World J Gastroenterol 11(3):344–347. https://doi.org/10.3748/wjg.v11.i3.34

Yan C, Li B, Fan F, Du Y, Ma R, Cheng XD, Li XY, Zhang B, Yu Q, Wang YG, Tang RX, Zheng KY (2017) The roles of Toll-like receptor 4 in the pathogenesis of pathogen-associated biliary fibrosis caused by *Clonorchis sinensis*. Sci Rep 7(1):3909. https://doi.org/10.1038/s41598-017-04018-8

Yip TC, Wong VW, Chan HL, Tse YK, Lui GC, Wong GL (2020) Tenofovir is associated with lower risk of hepatocellular carcinoma than entecavir in patients with chronic HBV INFection in China. Gastroenterology 158(1):215-225.e6. https://doi.org/10.1053/j.gastro.2019.09.025

Zhao Q, Yu WL, Lu XY, Dong H, Gu YJ, Sheng X, Cong WM, Wu MC (2016) Combined hepatocellular and cholangiocarcinoma originating from the same clone: a pathomolecular evidence-based study. Chin J Cancer 35(1):82. https://doi.org/10.1186/s40880-016-0146-7

Zhao H, Wu L, Yan G, Chen Y, Zhou M, Wu Y, Li Y (2021) Inflammation and tumor progression: signaling pathways and targeted intervention. Signal Transduct Target Ther 6(1):263. https://doi.org/10.1038/s41392-021-00658-5

Zheng S, Zhu Y, Zhao Z, Wu Z, Okanurak K, Lv Z (2017) Liver fluke infection and cholangiocarcinoma: a review. Parasitol Res 116(1):11–19. https://doi.org/10.1007/s00436-016-5276-y